Superconductivity and local-moment magnetism in $Eu(Fe_{0.89}Co_{0.11})_2As_2$

Shuai Jiang, Hui Xing, Guofang Xuan, Zhi Ren, Cao Wang, Zhu-an Xu, and Guanghan Cao*
Department of Physics, Zhejiang University, Hangzhou 310027, China

(Received 29 September 2009; revised manuscript received 29 October 2009; published 24 November 2009)

We report the measurements of resistivity and magnetization under magnetic fields parallel and perpendicular to the basal plane, respectively, on a cobalt-doped $Eu(Fe_{0.89}Co_{0.11})_2As_2$ single crystal. We observed a resistivity drop at $T_c \sim 21$ K, which shifts toward lower temperatures under external fields, suggesting a superconducting transition. The upper critical fields near T_c show large anisotropy, in contrast with those of other "122" FeAs-based superconductors. Low-field magnetic susceptibility data also show evidence of superconductivity below 21 K. Instead of the expected zero resistance below T_c, however, a resistivity re-entrance appears at 17 K under zero field, coincident with the magnetic ordering of Eu^{2+} moments. Based on the temperature and field dependences of anisotropic magnetization, a helical magnetic structure for the Eu^{2+} spins is proposed. External magnetic fields easily change the helimagnetism into ferromagnetism with fully polarized Eu^{2+} spins, accompanying by disappearance of the resistivity re-entrance. Therefore, superconductivity coexists with ferromagnetic state of Eu^{2+} spins under relatively low magnetic field. The magnetic and superconducting phase diagrams are finally summarized for both $H \parallel ab$ and $H \parallel c$.

DOI: 10.1103/PhysRevB.80.184514 PACS number(s): 74.70.Dd, 74.25.−q, 75.30.−m

I. INTRODUCTION

Superconductivity (SC) and ferromagnetism (FM) are mutually antagonistic cooperative phenomena, because superconducting state expels magnetic flux (Meissner effect) but FM generates the internal magnetic field. On one hand, the internal field generated by FM destroys SC in two ways: orbital effect[1] and paramagnetic effect (in the case of spin-singlet SC).[2] On the other hand, SC does not favor FM since SC state suppresses the zero wave-vector component of the electronic susceptibility, $\chi(0)$, which is crucial to mediate the localized moments via the Ruderman-Kittel-Kasuya-Yosida (RKKY) interaction. The incompatible nature of SC and local-moment FM was demonstrated in $ErRh_4B_4$ (Ref. 3) and $Ho_{1.2}Mo_6S_8$ (Ref. 4) which show the destruction of SC at the onset of long-range magnetic order. Later the repulsive effects between SC and FM were observed in a family of layered compounds RNi_2B_2C (R=Tm, Er, Ho, and Dy).[5] The interplay between SC and FM was also reported in Ru-layer-containing cuprates, where magnetic ordering temperatures are much higher than SC transition temperatures.[6,7] Interestingly, SC and local-moment[8] FM could be reconciled by considering their difference in interaction length scale. Earlier theoretical work[9] pointed out that SC could coexist with modulated FM such as spiral/helical magnetic configuration or multidomain structure. Later, it was theoretically shown that SC could be in the form of spontaneous vortex state[10,11] to facilitate the FM ordering. However, there have been few experimental evidences on how SC coexists with the FM.[12]

Doped $EuFe_2As_2$ system is another candidate for searching the coexistence of SC and local-moment FM. This material consists of two subsystems: (1) anti-fluorite-type Fe_2As_2 layers responsible for occurrence of superconductivity and (2) local-moment-carrying Eu^{2+} ions sandwiched by the Fe_2As_2 layers. In the undoped parent compound $EuFe_2As_2$, the two subsystems undergo an antiferromagnetic (AFM) spin-density wave (SDW) transition associated with Fe moments at 190 K and another AFM ordering for Eu^{2+} spins at 19 K, respectively.[13–16] The magnetic structure of the latter AFM order was proposed to be of A type,[17] in which Eu^{2+} spins align ferromagnetically in the basal planes but antiferromagnetically along the c axis, based on the anisotropic magnetic and magnetotransport measurements. This magnetic structure was very recently confirmed by the magnetic resonant x-ray scattering[18] and neutron diffraction[19] experiments.

By the partial substitution of Eu with K, SC over 30 K was reported in $Eu_{1-x}K_xFe_2As_2$.[20] However, no magnetic ordering for Eu^{2+} spins was observed, probably due to the dilution effect by the Eu-site doping. In the case of Fe-site doping, although superconductivity at 20 K was obtained in $BaFe_{2-x}Ni_xAs_2$,[21] attempt to obtain SC in $EuFe_{2-x}Ni_xAs_2$ was unsuccessful.[22] Instead, the Ni doping leads to FM ordering for the Eu^{2+} moments. By phosphorus doping at the As site, which also keeps Eu^{2+} sublattice undisturbed, we found bulk SC at T_c=26 K followed by a local-moment FM at 20 K in $EuFe_2(As_{0.7}P_{0.3})_2$.[23] In fact, with applying pressure, superconductivity at 29 K was reported in the undoped $EuFe_2As_2$,[24,25] where the AFM ordering for Eu^{2+} moments was proposed. The above results suggest that the prerequisite for finding the coexistence of SC and local-moment magnetism in Eu-containing arsenides is that T_c should be higher than the magnetic ordering temperature T_M. Note that the maximum T_c in $BaFe_{2-x}Co_xAs_2$ is as high as 25 K (Ref. 26); therefore, we investigated the $Eu(Fe_{1-x}Co_x)_2As_2$ system. Consequently, evidence of SC transition was observed for $0.09 \leq x < 0.15$, basically consistent with a very recent report by Zheng *et al.*[27]

In this paper, we present detailed measurements of the resistivity and magnetization under magnetic fields using well-characterized single crystals of $Eu(Fe_{0.89}Co_{0.11})_2As_2$. We observed a resistivity drop at 21 K for both in-plane (ρ_{ab}) and out-of-plane (ρ_c) resistivities, which is ascribed to a SC transition. Evidence of superconductivity is also given by low-field magnetic susceptibility measurement. Followed by the SC transition, a resistivity re-entrance appears as the Eu^{2+} spins order spontaneously. By analyzing the temperature and

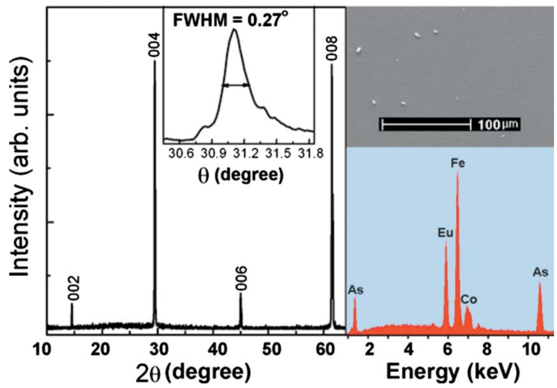

FIG. 1. (Color online) Characterizations of a Co-doped $EuFe_2As_2$ crystal in the present study by x-ray diffraction (left), scanning electron microscope (upper right), and energy dispersive x-ray spectroscopy (bottom right).

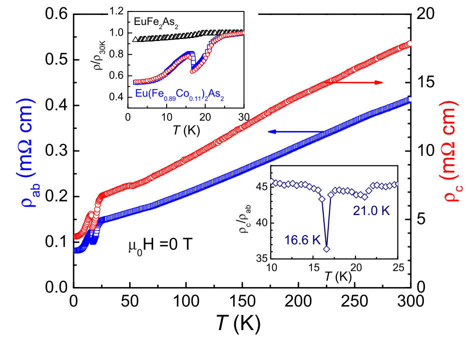

FIG. 2. (Color online) Temperature dependence of in-plane and out-of-plane resistivities for $Eu(Fe_{0.89}Co_{0.11})_2As_2$ crystals at zero field. Upper left inset is an expanded plot in comparison with the data of the nonsuperconducting $EuFe_2As_2$ crystals. Lower right inset displays the anisotropic ratio ρ_c/ρ_{ab}, showing two peaks associated with superconducting and magnetic transitions, respectively.

field dependences of anisotropic magnetization, and comparing with the magnetic structure of $EuFe_2As_2$, a helical magnetic structure for Eu^{2+} spins was proposed. External magnetic field reorientates the Eu^{2+} moments easily, changing the helimagnetism (HM) into ferromagnetism. Finally, the magnetic and superconducting phase diagrams were established, exhibiting the intriguing coexistence of SC and long-range magnetic ordering in $Eu(Fe_{0.89}Co_{0.11})_2As_2$.

II. EXPERIMENTAL

Single crystals of $Eu(Fe_{1-x}Co_x)_2As_2$ were grown using (Fe,Co)As as the self-flux, similar to previous reports.[17,28] (Fe,Co)As with the atomic ratio $Fe:Co=(1-x):x$ was presynthesized by reacting Fe powders with As shots in vacuum at 773 K for 6 h and then at 1030 K for 12 h. Fresh Eu grains and $Fe_{1-x}Co_xAs$ powders were thoroughly mixed in a molar ratio of 1:4. The mixture was loaded into an alumina tube then put into a quartz ampoule. The sealed quartz ampoule was heated to 1053 K at a heating rate of 150 K/h holding at this temperature for 10 h. Subsequently, the temperature was raised to 1398 K in 3 h holding for 5 h. The crystals were grown by slowly cooling to 1223 K at a cooling rate of 2 K/h. Finally, the quartz ampoule was cooled to room temperature by shutting off the furnace. Many shiny platelike crystals with the typical size of $3\times2\times0.1$ mm^3 were obtained.

The crystals were characterized by x-ray diffraction (XRD) and field-emission scanning electron microscopy (SEM), and energy dispersive x-ray (EDX) spectroscopy. XRD was performed using a D/Max-rA diffractometer with Cu $K\alpha$ radiation and a graphite monochromator. SEM image was taken in a field-emission scanning electron microscope (Sirion FEI, The Netherlands) equipped with a Phoenix EDAX x-ray spectrometer. Figure 1 shows the morphological, compositional, and structural characterizations on a Co-doped $EuFe_2As_2$ crystal. The SEM image of the crystal measured shows large area of flat surfaces with only minor impurities adhered to. Quantitative analysis for the EDX spectra indicates that the composition is $Eu(Fe_{0.89}Co_{0.11})_2As_2$ within the measurement error ($\pm5\%$). XRD pattern of $\theta-2\theta$ scan shows only (00l) reflections, indicating that the c axis is perpendicular to the crystal sheet planes. The c axis was calculated to be 1.207 nm, which is reasonably smaller than that of $EuFe_2As_2$.[14] The rocking curve (θ scan) shown in the inset has a relatively small full width at half maximum, suggesting high quality of the sample.

Electrical resistivity was measured using a standard four-terminal method. The electrode configuration in Ref. 28 was employed for measuring ρ_c. The dc magnetization was measured on a Quantum Design magnetic property measurement system (MPMS-5). The crystal was carefully mounted on a sample holder, with the applied field perpendicular or parallel to the crystallographic c axis. The deviation angle was estimated to be less than 5°.

We found that the SDW transition in the parent compound was suppressed with the Co doping, like the cases in other iron arsenides.[26,29] For $0.09\le x<0.15$, resistivity drop due to a SC transition was observed around 20 K. The sample of $x=0.09$ showed a resistivity upturn at 30 K due to the residual SDW transition. For the sample with $x=0.11$, no clear evidence of SDW transition could be observed. Compared with the $Ba(Fe_{1-x}Co_x)_2As_2$ system,[26] the optimal doping level in $Eu(Fe_{1-x}Co_x)_2As_2$ shifts to a larger value. In this paper we focus on the physical property measurements for the optimally doped sample with $x=0.11$.

III. RESULTS AND DISCUSSION

A. Resistivity

Figure 2 shows ρ_{ab} and ρ_c for $Eu(Fe_{0.89}Co_{0.11})_2As_2$ crystals under zero field. While ρ_c is nearly 50 times larger than ρ_{ab}, their temperature dependences are almost the same. At high temperatures both show usual metallic behavior. Around 20 K the resistivity drops by over 30%, suggesting a SC transition. However, it increases sharply below $T_{ret}=17$ K (T_{ret} denotes the resistivity re-entrance temperature), and a resistivity peak appears at 16 K. One notes that the resistivity maximum is still much lower than that of the undoped $EuFe_2As_2$, as shown in the upper inset of Fig. 2. This implies that the state around 16 K is still within the SC

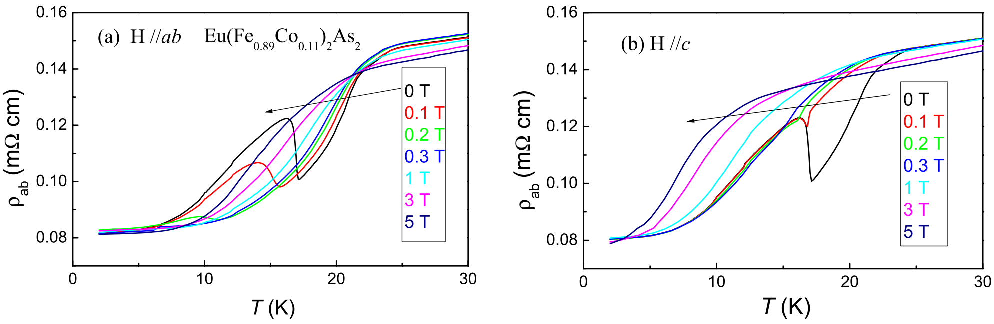

FIG. 3. (Color online) Resistive transition under magnetic fields for $Eu(Fe_{0.89}Co_{0.11})_2As_2$ crystals. (a) $H \| ab$; (b) $H \| c$.

regime. At lower temperatures, the resistivity tends to saturate at a residual value. This result resembles the behavior of $EuFe_2As_2$ under high pressures,[24] which was ascribed as a re-entrant superconductivity. The two transitions can also be manifested by the anomalous peaks in ρ_c/ρ_{ab}, shown in the lower inset of Fig. 2.

To clarify the above two resistivity anomalies, we performed the magnetoresistance (MR) measurements. Figure 3(a) shows the in-plane resistivity under magnetic fields parallel to the basal planes (hereafter denoted by $H \| ab$). As expected for a SC transition, the resistivity drop shifts to lower temperatures with increasing magnetic fields. On the other hand, the resistivity peak is drastically suppressed by the applied fields. When the applied field is perpendicular to the basal planes, as shown in Fig. 3(b), the SC transition is suppressed more severely by the field. However, the resistivity peak is not influenced very much until it is "buried" by the SC transition. The inset of Fig. 4 clearly shows the different responses of T_{ret} to the applied field along different directions. This observation is in sharp contrast with that in $RNi_2B_2C_2$ superconductors,[5] where the re-entrant region becomes much enlarged by the external field.

From the magnetoresistivity data, the upper critical fields were determined by using the criterion of 90% normal-state resistivity. As shown in Fig. 4, upward curvature can be seen in the $H_{c2}(T)$ curves, especially for $H \perp ab$. The anisotropic ratio, $H_{c2}^{\|}/H_{c2}^{\perp}$, achieves 30 at ~17 K. This contrasts with the nearly isotropic H_{c2} in $BaFe_2As_2$.[30] The large anisotropy in H_{c2} reflects the interplay between SC and magnetic orderings of Eu^{2+} moments. The initial slope $\mu_0 \partial H_{c2}^{\|}/\partial T$ near T_c is -1.3 T/K, giving an upper critical field of

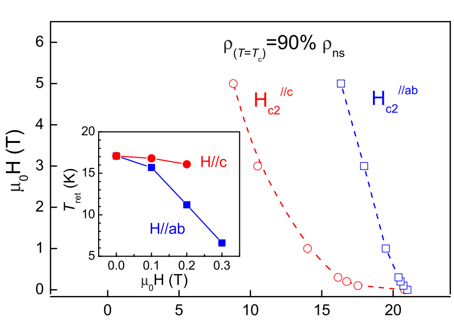

FIG. 4. (Color online) Upper critical fields of $Eu(Fe_{0.89}Co_{0.11})_2As_2$ single crystals. Inset: resistivity re-entrance temperature T_{ret} as a function of applied field.

$\mu_0 H_{c2}^{\|}(0) \sim 26$ T by linear extrapolation. This upper critical field is obviously lower than the Pauli paramagnetic limit $\mu_0 H_P = 1.84 T_c \approx 38.6$ T. The situation is similar to that in the $EuFe_2(As_{0.7}P_{0.3})_2$ superconductor,[23] but different from those of other Eu-free ferroarsenide superconductors.[31] The lower magnitude of $H_{c2}(0)$ especially in Eu-containing superconductors implies the existence of significant internal field from the Eu^{2+} moments.

Figure 5 shows the isothermal resistivity under magnetic field parallel or perpendicular to the basal planes. At 30 K, the resistivity decreases monotonically with the field. Negative MR was also observed in $EuFe_2As_2$ just above the Eu-AFM ordering temperature,[17] which was ascribed to the reduction in Eu-spin disorder scattering by the external magnetic field. At 21 and 17 K, an abrupt increase in resistivity at relatively low fields, especially for $H \perp ab$, is observed, representing the transition from superconductivity to normal state. The normal-state $\rho_{ab}^{\|}$ increases with the field, which reflects the intrinsic transport property of FeAs layers

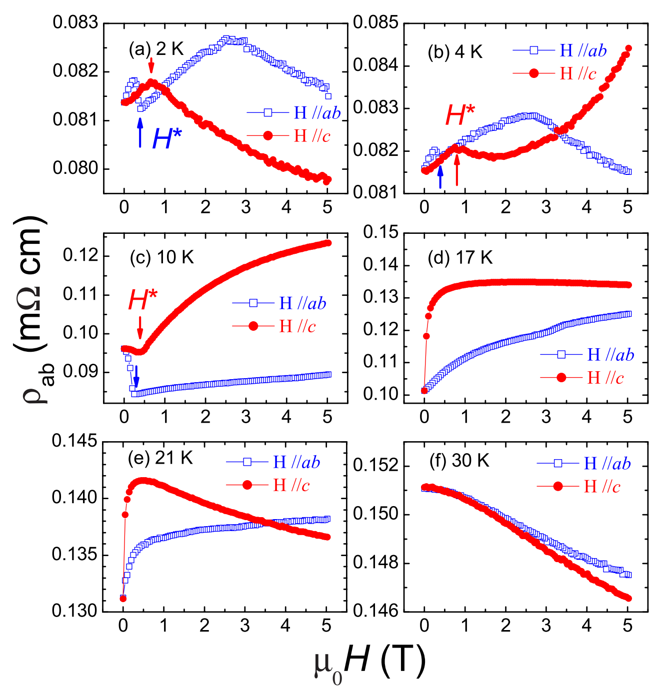

FIG. 5. (Color online) Field dependence of in-plane resistivity in $Eu(Fe_{0.89}Co_{0.11})_2As_2$ at fixed temperatures. The turning in resistivity at H^* is marked by arrows.

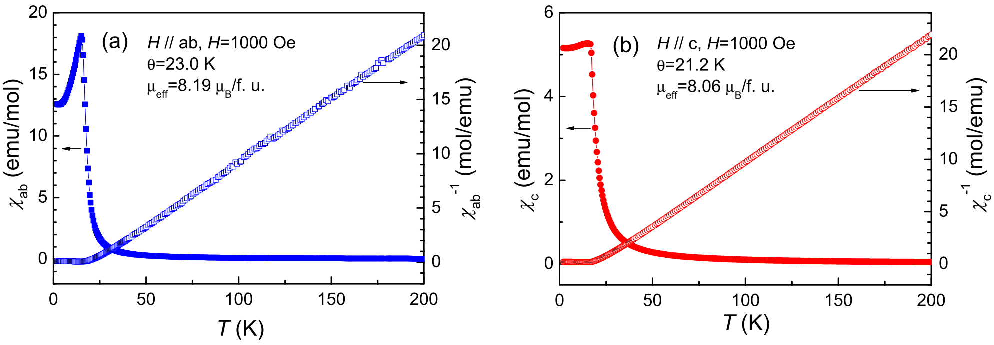

FIG. 6. (Color online) Temperature dependence of magnetic susceptibility for $Eu(Fe_{0.89}Co_{0.11})_2As_2$. The measurements were performed in field cooling mode under the applied field of 1000 Oe. (a) $H \| ab$; (b) $H \| c$.

because of field-induced ferromagnetic transition. At 10 K, SC coexists with the helical magnetic order (see the next section) at low fields. The resistivity first decreases to a minimum at H^* then increases again with the field. The decrease in ρ_{ab} is related to the reorientation of Eu^{2+} moments, because $H^*=H_s$ (H_s refers to the saturated field; see Fig. 9 in the next section). The increase in ρ_{ab} is probably due to the increase in SC vortices by the external field and/or the intrinsic transport property of FeAs layers. At 2 and 4 K, $\rho_{ab}^{\perp}$ first increases to a maximum at H^* and then starts to decrease with the field. In the case of $H \| ab$, $\rho_{ab}^{\|}$ first increases also, then decreases to a minimum at $H^*=H_s$. Interestingly, another maximum appears at higher field. These data should reflect the interplay between SC and magnetism, but we fail to have a sound explanation at present. The nonzero resistance is probably due to the dissipation of the motion of spontaneous vortex, generated by the magnetic ordering of Eu^{2+} spins. However, such spontaneous vortex should be directly evidenced before a quantitative understanding.

B. Magnetic properties

Figure 6 shows the temperature dependence of magnetic susceptibility. The high-temperature susceptibility well obeys the Curie-Weiss behavior: $\chi=\chi_0+C/(T-\theta)$, where χ_0 denotes the temperature-independent term, C is the Curie-Weiss constant, and θ is the paramagnetic Curie temperature. The data fitting ($50<T<200$ K) shows that the effective moment is close to the theoretical value $g\sqrt{S(S+1)}\mu_B=7.94\mu_B$ ($S=7/2$ and $g=2$) for a free Eu^{2+} ion. The θ values are positive, suggesting ferromagnetic interaction among Eu^{2+} spins.

Although the high-temperature susceptibility is basically isotropic, χ_{ab} is obviously higher than χ_c at low temperatures, e.g., χ_{ab}/χ_c is about 3.5 at 17 K. This suggests that the easy magnetization direction is parallel to the ab planes, similar to the case in $EuFe_2As_2$.[17] Below $T_M=17$ K, χ_{ab} decreases rather sharply, indicating an antiferromagneticlike transition. On the other hand, χ_c remains nearly constant below T_M. Therefore, one concludes that the Eu^{2+} moments are perpendicular to the c axis below T_M. Considering the dominant ferromagnetic interaction among Eu^{2+} spins, one expects ferromagnetic arrangement for the Eu^{2+} spins within single Eu^{2+} layer. This is quite similar to the situation in $EuFe_2As_2$ (Ref. 17); in latter case the magnetic ordering temperature is 2 K higher.

However, we note that the magnitude of drop in χ_{ab} is much smaller, compared with $EuFe_2As_2$ crystals.[17] The residual susceptibility at zero temperature is about 2/3 of χ_{max} at T_M, irrespective of changing the relative orientation between the sample and the applied field within ab planes. In addition, the field dependence of magnetization shows only a spin reorientation process for $H \| ab$ (see Fig. 9), in contrast with the steplike magnetization curves in $EuFe_2As_2$.[17] Both results suggest the noncollinear alignment for Eu^{2+} spins, although lying in the ab planes. Therefore, we propose a helical magnetic order for Eu^{2+} moments in $Eu(Fe_{0.89}Co_{0.11})_2As_2$, i.e., the moments of the neighboring FM Eu^{2+} layers form an angle of φ ($\varphi \neq n\pi$, where n is an integer). Such a noncollinear magnetic order was first observed in the 1950s in $MnAu_2$,[32] in which the FM basal planes of Mn atoms are sandwiched by two layers of Au atoms.

The Eu-interlayer spacing is so large that interlayer magnetic coupling should be an indirect RKKY interaction, which has much longer range and changes its sign with the distance and Fermi wave vector. In the framework of RKKY interaction, the above noncollinear HM is possible if considering both nearest-neighboring and next-nearest-neighboring (along the c axis) interlayer couplings. According to a simplified derivation,[33]

$$\cos \varphi = -\frac{J_{NN}}{4J_{NNN}}. \tag{1}$$

The above solution corresponds to helimagnetic order, when $|J_{NN}|<|4J_{NNN}|$. Here, we note that the HM is compatible with the SC order, as theoretical work[9] pointed out.

Due to the proximity of superconducting transition and magnetic ordering, the superconducting diamagnetic signal could be very weak. The huge paramagnetic background from Eu^{2+} spins also makes it difficult to directly observe the diamagnetism. To find the signal of SC, we carried out the low-field susceptibility measurement, as shown in Fig. 7. For $H \| ab$, the magnetic transition temperature decreases even by a small field of 500 Oe. When the field is less than 10 Oe, an increase in χ can be observed at 13 K. Such an anomaly is

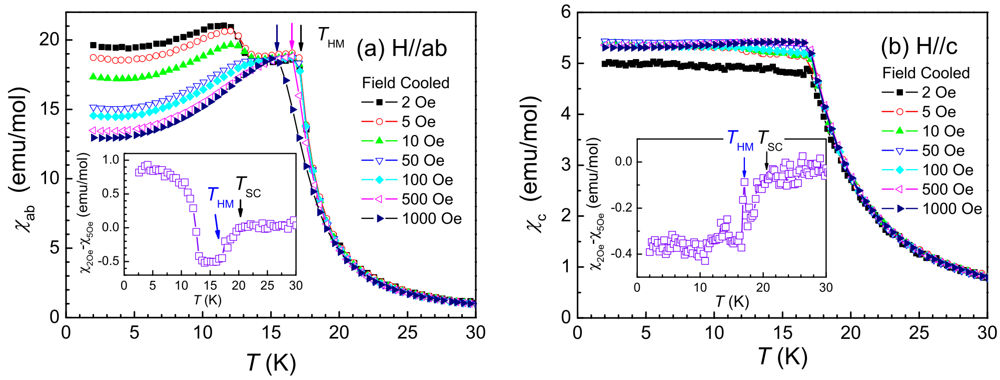

FIG. 7. (Color online) Low-field magnetic susceptibility for $Eu(Fe_{0.89}Co_{0.11})_2As_2$. The insets make a subtraction: $\Delta\chi=\chi_{2\ \mathrm{Oe}}-\chi_{5\ \mathrm{Oe}}$. The superconducting temperature T_{SC} and the helical magnetic ordering temperature T_{HM} are marked. (a) $H\|ab$; (b) $H\|c$.

pronounced with decreasing field. Thus, we made a subtraction: $\Delta\chi=\chi_{2\ \mathrm{Oe}}-\chi_{5\ \mathrm{Oe}}$, as shown in the inset. One sees an abrupt decrease at 21 K, corresponding to the resistivity drop in Fig. 2. This result is reproducible for the subtractions using different $\chi_H(T)$ data. Furthermore, the subtraction of $\chi_{FC}(T)$ from $\chi_{ZFC}(T)$ also gives evidence of SC below 21 K. The "diamagnetism" in the paramagnetic background suggests SC in $Eu(Fe_{0.89}Co_{0.11})_2As_2$. The absence of bulk Meissner effect, similar to the case in $EuFe_2(As_{0.7}P_{0.3})_2$,[23] should be associated with the magnetic ordering of Eu^{2+} spins. Theoretical work[34] indicates that, in the limit of large saturated magnetic moment and magnetic anisotropy, there will be no Meissner effect. In that case, the effective lower critical field H_{c1} will be zero and superconductivity appears only when vortices are pinned to impurity sites. In fact, the above difference in $\chi_H(T)$ for $H=2$ and 5 Oe suggests that H_{c1} is really much lower than expected.

Here, we have to address another anomaly in $\Delta\chi$, i.e., the increase at 13 K. This phenomenon is reminiscent of paramagnetic Meissner effect (PME). Intrinsic PME can be produced from a spontaneous flux in a SC loop made of Josephson junction with superconducting phase difference.[35] In the SC and HM coexisted state, similar junctions can be possibly formed due to the proximity effect in SC-FM boundaries.[36] Therefore, spontaneous flux could be generated mostly parallel to *ab* planes. This could result in the observed PME for $H\|ab$. In the case of $H\perp ab$, the SC transition at 21 K can also be clearly seen. However, the PME-like transition is not so obvious, consistent with the spontaneous flux perpendicular to the *c* axis.

Figure 8 shows the temperature dependence of magnetization under fixed magnetic fields. For both $H\|ab$ and $H\perp ab$, T_{HM} decreases with the field. Compared with $T_{HM}^{\perp}$, $T_{HM}^{\|}$ is more easily suppressed by the magnetic fields. The variations of T_{HM} coincide with the changes in T_{ret} (shown in Fig. 3), suggesting that the resistivity re-entrance is closely related to the helimagnetic transitions. The decrease in T_{HM} by external fields can be qualitatively understood in terms of the above simple model considering the interlayer magnetic couplings J_{NN} and J_{NNN}. Under magnetic fields, the effective coupling is modified as $J_{eff}=J+J_{ext}$ (J_{ext} denotes the contribution from the applied field). Thus, the applied field possibly makes the inequality $|J_{NN,eff}|<|4J_{NNN,eff}|$ invalid (note that $|J_{NN,eff}|=|J_{NN}+J_{ext}|$, $|4J_{NNN,eff}|=4|J_{NNN}+J_{ext}|$), leading to the appearance of a more stabilized FM phase.

Under higher magnetic field, the HM-FM transition can be verified by the saturation of magnetization to a fully polarized value $gS=7.0\mu_B$/f.u. ($g=2$ and $S=7/2$). Here, we identify the FM transition temperature T_{Curie} as the inflection point of the $M(T)$ curves. The derivative of magnetization, plotted in the inset of Fig. 8, indicates that T_{Curie} increases with the field.

Figure 9 shows the isothermal magnetization for the $Eu(Fe_{0.89}Co_{0.11})_2As_2$ crystals. At 2 K, the magnetization in-

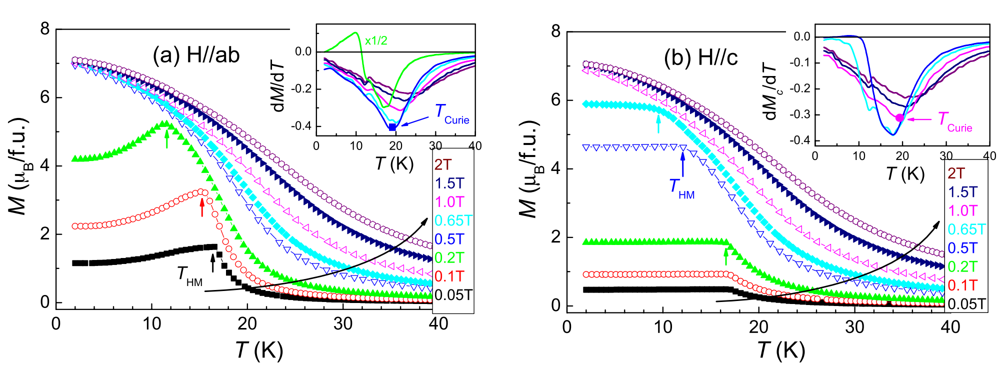

FIG. 8. (Color online) Temperature dependence of magnetization at fixed magnetic fields for $Eu(Fe_{0.89}Co_{0.11})_2As_2$ crystals. The arrows mark the helimagnetic ordering temperature. The inset plots the derivative of magnetization, showing the ferromagnetic transitions at T_{Curie}. (a) $H\|ab$; (b) $H\|c$.

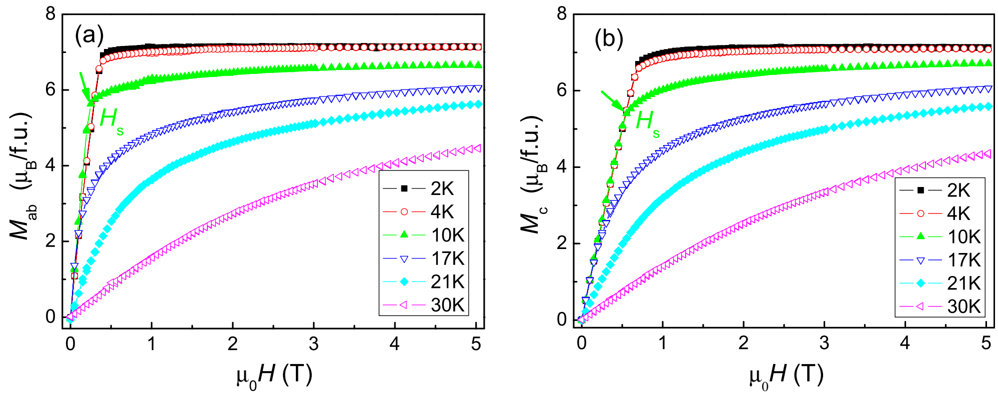

FIG. 9. (Color online) Field dependence of magnetization at fixed temperatures for $Eu(Fe_{0.89}Co_{0.11})_2As_2$ crystals. The saturated field H_s is marked by the arrow. (a) $H \parallel ab$; (b) $H \parallel c$.

creases almost linearly until achieving the saturated value of $7.0\mu_B$/f.u. for both directions of magnetic fields. The $M_c(H)$ behavior resembles that of $EuFe_2As_2$, except for the smaller saturated field $H_s^{\perp}$. However, the $M_{ab}(H)$ curve is qualitatively different from its counterpart of $EuFe_2As_2$ crystals. The latter shows a steplike magnetization at 2 K, which was identified as a metamagnetic transition associated with a spin-flip process.[17] Since the spin flip is related to the A-type antiferromagnetic structure, the absence of steplike magnetization in $Eu(Fe_{0.89}Co_{0.11})_2As_2$ points to the helimagnetic structure proposed above.

The magnetic state of Eu^{2+} moments correlates with the $\rho(H)$ data shown in Fig. 5. At $H=H_s=H^*$ and $T<17$ K, a turning point can also be found in the $\rho(H)$ curve. This observation reveals the interplay between SC and the magnetism of Eu^{2+}. For $H>H_s$, the Eu^{2+} spins are fully aligned along the magnetic field. Thus, the magnetic state is basically homogeneous. Under this circumstance, superconductivity could survive in the form of superconducting vortices. The electric current through the sample will result in the dissipative motion of the vortex, thus showing nonzero resistance. In the HM state ($H<H_s$), one expects noncollinear vortex, which could lead to a possibly larger dissipation. This is a plausible explanation we can figure out at present for the resistivity re-entrance shown in Fig. 3.

C. Phase diagram

Based on the above experimental results, the magnetic and superconducting phase diagrams were summarized as shown in Fig. 10. There are five different types of phase regimes. The first is paramagnetic normal state, located at the upper region in the phase diagrams. The second is paramagnetic superconducting state, which has a small area with narrow ranges of temperature and field. In the third state, located at the lower left side, SC coexists with the helimagnetic ordering of Eu^{2+} moments. The fourth is FM normal state, stabilized by external magnetic fields. The last phase shows the coexistence of SC and FM states, where spontaneous vortex phase is expected. As can be seen, the phase boundaries are obviously different for $H \parallel ab$ and $H \parallel c$. However, both cases show five states in terms of magnetic ordering of Eu^{2+} spins and SC associated with Fe 3d electrons.

IV. CONCLUDING REMARKS

In summary, we have measured the resistivity and magnetization under magnetic fields on $Eu(Fe_{0.89}Co_{0.11})_2As_2$ single crystals. Evidence of superconducting transition at 21 K was given from low-field magnetic susceptibility as well

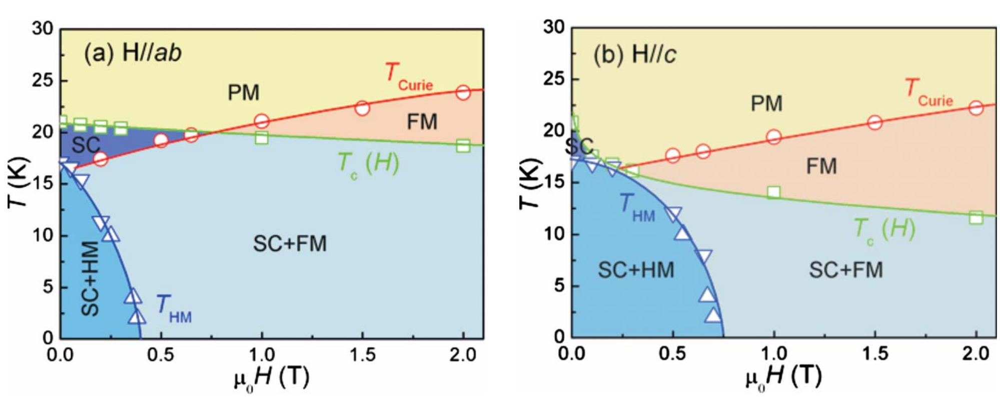

FIG. 10. (Color online) Electronic phase diagrams in $Eu(Fe_{0.89}Co_{0.11})_2As_2$. PM: paramagnetic state; SC: superconducting state; FM: ferromagnetic state; SC+HM: coexistence of superconductivity and helimagnetic order; SC+FM: coexistence of superconductivity and ferromagnetic state. (a) $H \parallel ab$; (b) $H \parallel c$.

as (magneto)resistivity. Below 17 K, Eu^{2+} moments are most likely helically ordered under low magnetic fields, which cause resistivity re-entrance. The Eu^{2+} moments can be easily reorientated by the external fields, exhibiting the coexistence of SC and FM states.

There are still some open questions in the present study. One is the origin of large nonzero resistance. While it is possible that spontaneous vortex accounts for the nonzero resistance, direct evidence of spontaneous vortex is called for. The other is the low-field magnetic susceptibility anomaly at 13 K. Whether it is truly a PME and is originated from spontaneous flux is of great interest. Here, we suggest that low-temperature magnetic force microscopy and scanning superconducting quantum interference device technique should be employed. Furthermore, specific electrical transport properties such as Hall and Nernst coefficients could be helpful to resolve the above issues.

ACKNOWLEDGMENTS

This work was supported by the NSF of China, National Basic Research Program of China (Contract No. 2007CB925001), and the PCSIRT of the Ministry of Education of China (Contract No. IRT0754).

*Corresponding author; ghcao@zju.edu.cn

[1] V. L. Ginzburg, Sov. Phys. JETP **4**, 153 (1957).
[2] D. Saint-James, G. Sarma, and E. J. Thomas, *Type II Superconductivity* (Pergamon, New York, 1969).
[3] W. A. Fertig, D. C. Johnston, L. E. DeLong, R. W. McCallum, M. B. Maple, and B. T. Matthias, Phys. Rev. Lett. **38**, 987 (1977).
[4] M. Ishikawa and O. Fischer, Solid State Commun. **23**, 37 (1977).
[5] H. Eisaki, H. Takagi, R. J. Cava, B. Batlogg, J. J. Krajewski, W. F. Peck, K. Mizuhashi, J. O. Lee, and S. Uchida, Phys. Rev. B **50**, 647 (1994).
[6] I. Felner, U. Asaf, Y. Levi, and O. Millo, Phys. Rev. B **55**, R3374 (1997).
[7] C. Bernhard, J. L. Tallon, Ch. Niedermayer, Th. Blasius, A. Golnik, E. Brucher, R. K. Kremer, D. R. Noakes, C. E. Stronach, and E. J. Ansaldo, Phys. Rev. B **59**, 14099 (1999).
[8] Here, we do not consider another important scenario in which SC and FM are formed by the same electrons. The example are shown in UGe_2 [S. S. Saxena, P. Agarwal, K. Ahilan, F. M. Grosche, R. K. W. Haselwimmer, M. J. Steiner, E. Pugh, I. R. Walker, S. R. Julian, P. Monthoux, G. G. Lonzarich, A. Huxley, I. Sheikin, D. Braithwaite, and J. Flouquet, Nature (London) **406**, 587 (2000)], where coexistence of triplet SC and weak itinerant FM was proposed.
[9] P. W. Anderson and H. Suhl, Phys. Rev. **116**, 898 (1959).
[10] H. S. Greenside, E. I. Blount, and C. M. Varma, Phys. Rev. Lett. **46**, 49 (1981).
[11] M. Tachiki, H. Matsumoto, T. Koyama, and H. Umezawa, Solid State Commun. **34**, 19 (1980).
[12] L. N. Bulaevskii, A. I. Buzdin, M. L. Kulic, and S. V. Panjukov, Adv. Phys. **34**, 175 (1985).
[13] R. Marchand and W. Jeitschko, J. Solid State Chem. **24**, 351 (1978).
[14] Z. Ren, Z. W. Zhu, S. Jiang, X. F. Xu, Q. Tao, C. Wang, C. M. Feng, G. H. Cao, and Z.-A. Xu, Phys. Rev. B **78**, 052501 (2008).
[15] H. S. Jeevan, Z. Hossain, D. Kasinathan, H. Rosner, C. Geibel, and P. Gegenwart, Phys. Rev. B **78**, 052502 (2008).
[16] D. Wu, N. Barisic, N. Drichko, S. Kaiser, A. Faridian, M. Dressel, S. Jiang, Z. Ren, L. J. Li, G. H. Cao, Z. A. Xu, H. S. Jeevan, and P. Gegenwart, Phys. Rev. B **79**, 155103 (2009).
[17] S. Jiang, Y. K. Luo, Z. Ren, Z. W. Zhu, C. Wang, X. F. Xu, Q. Tao, G. H. Cao, and Z.-A. Xu, New J. Phys. **11**, 025007 (2009).
[18] J. Herrero-Martin, V. Scagnoli, C. Mazzoli, Y. Su, R. Mittal, Y. Xiao, Th. Bruckel, N. Kumar, S. Dhar, A. Thamizhavel, and L. Paolasini, Phys. Rev. B **80**, 134411 (2009).
[19] Y. Xiao, Y. Su, M. Meven, R. Mittal, C. Kumar, T. Chatterji, S. Price, J. Persson, N. Kumar, S. Dhar, A. Thamizhavel, and Th. Brueckel, arXiv:0908.3142 (unpublished).
[20] H. S. Jeevan, Z. Hossain, D. Kasinathan, H. Rosner, C. Geibel, and P. Gegenwart, Phys. Rev. B **78**, 092406 (2008).
[21] L. J. Li, Y. K. Luo, Q. B. Wang, H. Chen, Z. Ren, Q. Tao, Y. K. Li, X. Lin, M. He, Z. W. Zhu, G. H. Cao, and Z. A. Xu, New J. Phys. **11**, 025008 (2009).
[22] Z. Ren, X. Lin, Q. Tao, S. Jiang, Z. W. Zhu, C. Wang, G. H. Cao, and Z.-A. Xu, Phys. Rev. B **79**, 094426 (2009).
[23] Z. Ren, Q. Tao, S. Jiang, C. M. Feng, C. Wang, J. H. Dai, G. H. Cao, and Z.-A. Xu, Phys. Rev. Lett. **102**, 137002 (2009).
[24] C. F. Miclea, M. Nicklas, H. S. Jeevan, D. Kasinathan, Z. Hossain, H. Rosner, P. Gegenwart, C. Geibel, and F. Steglich, Phys. Rev. B **79**, 212509 (2009).
[25] T. Terashima, M. Kimata, H. Satsukawa, A. Harada, K. Hazama, S. Uji, H. S. Suzuki, T. Matsumoto, and K. Murada, J. Phys. Soc. Jpn. **78**, 083701 (2009).
[26] X. F. Wang, T. Wu, G. Wu, R. H. Liu, H. Chen, Y. L. Xie, and X. H. Chen, New J. Phys. **11**, 045003 (2009); K. Terashima, Y. Sekiba, J. H. Bowen, K. Nakayama, T. Kawahara, T. Sato, P. Richard, Y.-M. Xu, L. J. Li, G. H. Cao, Z.-A. Xu, H. Ding, and T. Takahashib, Proc. Natl. Acad. Sci. U.S.A. **106**, 7330 (2009).
[27] Q. Zheng, Y. He, T. Wu, G. Wu, H. Chen, J. Ying, R. Liu, X. Wang, Y. Xie, Y. Yan, Q. Li, and X. Chen, arXiv:0907.5547 (unpublished).
[28] X. F. Wang, T. Wu, G. Wu, H. Chen, Y. L. Xie, J. J. Ying, Y. J. Yan, R. H. Liu, and X. H. Chen, Phys. Rev. Lett. **102**, 117005 (2009).
[29] A. S. Sefat, A. Huq, M. A. McGuire, R. Y. Jin, B. C. Sales, D. Mandrus, L. M. D. Cranswick, P. W. Stephens, and K. H. Stone, Phys. Rev. B **78**, 104505 (2008); C. Wang, Y. K. Li, Z. W. Zhu, S. Jiang, X. Lin, Y. K. Luo, S. Chi, L. J. Li, Z. Ren, M. He, H. Chen, Y. T. Wang, Q. Tao, G. H. Cao, and Z. A. Xu, *ibid.* **79**, 054521 (2009).
[30] H. Q. Yuan, J. Singleton, F. F. Balakirev, S. A. Baily, G. F. Chen, J. L. Luo, and N. L. Wang, Nature (London) **457**, 565 (2009).

[31] G. H. Cao, S. Jiang, X. Lin, C. Wang, Y. K. Li, Z. Ren, Q. Tao, C. M. Feng, J. H. Dai, Z. A. Xu, and F. C. Zhang, Phys. Rev. B **79**, 174505 (2009); C. Wang, S. Jiang, Q. Tao, Z. Ren, Y. K. Li, L. J. Li, C. M. Feng, J. H. Dai, G. H. Cao, and Z. A. Xu, EPL **86**, 47002 (2009); Q. Tao, J. Q. Shen, L. J. Li, X. Lin, Y. K. Luo, G. H. Cao, and Z. A. Xu, Chin. Phys. Lett. **26**, 097401 (2009).

[32] A. Herpin, Acad. Sci., Paris, C. R. **246**, 3170 (1958); **249**, 1334 (1959).

[33] S. Blundell, *Magnetism in Condensed Matter* (Oxford University Press, New York, 2001).

[34] T. K. Ng and C. M. Varma, Phys. Rev. Lett. **78**, 330 (1997).

[35] D. Dominguez, E. A. Jagla, and C. A. Balseiro, Phys. Rev. Lett. **72**, 2773 (1994).

[36] A. I. Buzdin, Rev. Mod. Phys. **77**, 935 (2005).